ANATOMICAL AND FUNCTIONAL ASSESSMENT OF CORONARY ARTERY DISEASE USING COMPUTED TOMOGRAPHY ANGIOGRAPHY

PhD thesis

Borbála Vattay, MD

Doctoral School of Theoretical and Translational Medicine
Semmelweis University

Supervisor: Bálint Szilveszter, MD, PhD

Official reviewers: Katalin Keltai, MD, PhD
Eszter Végh, MD, PhD
Head of the Complex Examination Committee:
István Karádi, MD, PhD, DSc
Members of the Complex Examination Committee:
Henriette Farkas, MD, PhD, DSc
Hassan Charaf, PhD, DSc
Miklós Kellermayer, MD, PhD, DSc

Budapest, 2025

1. Introduction

Cardiovascular diseases, including coronary artery disease (CAD), remain the leading cause of mortality worldwide and impose a significant burden on healthcare systems. While mortality from myocardial infarction and stroke has decreased in Hungary over the past 15 years, deaths from other ischemic heart diseases have doubled, underscoring the importance of prevention and early detection. Established risk scores (e.g. SCORE2, ASCVD) rely on traditional risk factors but may fail to identify all high-risk individuals due to changing population health trends. CAD is a chronic and dynamic process with often asymptomatic progression, and initial presentation may be acute coronary syndrome or sudden cardiac death. Non-invasive imaging, particularly coronary computed tomography angiography (CTA), has gained a central role in early detection and risk stratification of CAD. Coronary CTA is now a class I recommended first-line diagnostic modality in chronic coronary syndrome (CCS), with high accuracy for ruling out obstructive CAD and assessing plaque burden and high-risk plaque (HRP) features. CTA allows anatomical and, using advanced techniques, functional evaluation of CAD. Quantitative plaque assessment enables the analysis of plaque composition and volume, which are increasingly recognized as independent predictors of cardiovascular events. Recent evidence highlights the importance of total coronary plaque burden - beyond luminal stenosis severity - in personalized prevention strategies. Functional assessment using dynamic myocardial perfusion CT (DPCT) complements anatomical data by detecting ischemia with high spatial resolution. Combining CTA and DPCT in a single exam allows for the simultaneous evaluation of coronary morphology and myocardial perfusion, enhancing clinical decision-making. The advent of photon-counting CT (PCCT) technology represents a breakthrough in cardiac imaging,

offering superior spatial resolution, noise reduction and improved tissue characterization. PCCT enables advanced plaque characterization and virtual monoenergetic imaging (VMI), which may affect quantitative plaque measurements.

2. Objectives

The objective of this thesis was to establish the following aims:

2.1 Defining coronary plaque progression using different definitions of coronary artery disease assessed by coronary CTA.

2.2 Defining the association between quantitative coronary plaque metrics and myocardial ischemia using CTA.

2.3 Defining the changes in quantitative coronary plaque characteristics using spectral CTA imaging.

3. Methods

3.1 Methods for plaque progression assessment

In this retrospective study we included patients who underwent serial coronary CTA (≥1-year interval) using the same 256-slice CT scanner (Philips Brilliance iCT). Exclusion criteria were prior myocardial infarction, revascularization, heart transplantation, or non-diagnostic image quality. Most patients underwent follow-up CTA for recurrent angina (76.6%) or pre-ablation evaluation of atrial fibrillation (23.4%). All CTA examinations were ECG-triggered and followed SCCT guidelines. Standardized protocols included beta-blocker and sublingual nitroglycerine administration for optimal image quality. Coronary plaques were evaluated in ≥1.5 mm segments based on established HU thresholds (≥130 HU for calcified, <130 HU for non-calcified). Plaque burden was defined by using segment involvement score (SIS), segment stenosis score (SSS) and CAD-RADS classification. Progression was defined as any increase in these metrics. Baseline and follow-up scans were

read simultaneously by a blinded observer. A paired sample t-test was used to compare parameters describing coronary plaque burden between the two CTA examinations. Linear mixed models were used to analyze repeated observations at non-standardized intervals. Univariate linear mixed models were calculated to assess the effect of each predictor on the outcome (CAD definitions) and its annual progression. Predictors with a p-value <0.10 in either effect were included in a multivariate model. Clinical predictors of coronary plaque progression were included as predictors, with SIS, SSS, and CAD-RADS as outcomes.

3.2 Methods for the association of quantitative plaque metrics and myocardial ischemia

In this prospective, single-center study, patients with stable chest pain and ≥30% stenosis detected on coronary CTA were enrolled. Exclusion criteria were prior myocardial infarction, revascularization, heart transplantation, contraindications to regadenoson, or inadequate image quality. Regadenoson stress DPCT was performed separately. Coronary CTA acquisition protocol was identical to previous substudy of the thesis described at section *3.1*. Stress DPCT was performed after rest CTA on the same scanner. Hyperemia was induced with a single 400 μg intravenous dose of regadenoson, and imaging was acquired during a single breath-hold at peak stress, one minute post-injection, covering 25-30 cardiac cycles. Prospective ECG-gated dynamic imaging was acquired in systole (35% R-R interval). Quantitative plaque analysis was performed on rest CTA images using a dedicated software (QAngioCT Research Edition v3.1; Medis Medical Imaging Systems). Coronary segments were defined by the 18-segment SCCT model and analyzed by a single blinded reader for vessels >1.5 mm. Plaques were classified by HU thresholds: LAP: -100-30; NCP: 31-350;

CP: ≥351. Volumes of total plaque and subcomponents were calculated, with LAP burden defined as LAP volume×100%/vessel volume. Lumen stenosis was measured at maximal narrowing, remodeling index (RI) was computed as the ratio of vessel wall area at the site of maximal luminal narrowing to the reference vessel wall area, and HRP as quantitative LAP burden >4% or a RI >1.1. DPCT images were analyzed using a dedicated software (Intellispace Portal; Philips Healthcare). Short-axis views were used for left ventricular myocardial assessment, and ROIs >0.5 cm^2 were placed in each myocardial segment using a 16-segment model. MBF was computed using hybrid deconvolution method, with two blinded readers independently analyzing segments. Myocardial ischemia was defined as MBF <101 ml/100 g/min. Relative MBF (MBFi) was calculated as absolute MBF/reference MBF (75th percentile of all MBF values for a given patient). In our segment-based approach, we defined coronary artery segments supplying each of the 16 analyzed myocardial segments based on dominance and segment location relative to basal, mid-ventricular, or apical regions. After adjudication, the TPV, NCP volume, and CP volume from all relevant supplying coronary segments were aggregated for each myocardial segment. An independent t-test was employed to compare parameters describing coronary plaque burden between ischemic and non-ischemic segments. Pearson correlation analysis was used to examine the associations between TPV, NCP, and CP volume. Linear and logistic mixed models, adjusting for intra-patient clustering and clinical factors, were utilized to assess the relationships between TPV, maximal area stenosis, quantitative HRP features, and absolute MBF, relative MBF (MBFi), or myocardial ischemia (defined as MBF < 101 ml/100 g/min).

3.3 Methods for quantitative plaque characterization using photon-counting CT

In this prospective, single-center study, consecutive patients undergoing clinically indicated coronary CTA for suspected or known CAD were screened. Inclusion required diagnostic image quality and ≥1 discernible lesion in a main coronary artery; patients with stents, bypass grafts, or severe artifacts were excluded. Coronary CTA was performed on a first-generation dual-source PCCT scanner (NAEOTOM Alpha, Siemens Healthineers) following SCCT guidelines. VMIs were reconstructed from 40-180 keV (in 10-keV increments), and polychromatic images at 120 kVp (T3D) were also generated as reference standard for comparison. Coronary plaque was analyzed on CTA using dedicated semi-automated software (AutoPlaque 2.5; Cedars-Sinai Medical Center) by a single experienced reader. The lesion with the greatest stenosis was selected per patient to mitigate potential intra-patient clustering effects. Vessel centerlines and plaque borders were defined on T3D images, with automated lumen/vessel wall contouring and manual correction as needed. Segmentation masks from T3D were applied across all VMIs to ensure to ensure uniform analysis of the same voxels. Voxel data from the corresponding images were exported to the R environment (version 4.0.2) and analyzed using the Radiomics Image Analysis software package (RIA v.1.6.0). Plaque volumes (CP, NCP, LAP) were calculated, with components defined by two established HU-threshold methods: Method 1: LAP: -100-30 HU; NCP: 30-350 HU; CP: >350 HU; Method 2: LAP: <30 HU; NCP: 30-130 HU; CP: >130 HU. To compare plaque volumes across different monoenergetic levels, we employed one-way repeated measures analysis of variance (ANOVA) followed by post hoc comparisons. Our analysis involved two main comparisons: (1) each VMI group versus T3D images to identify significant

differences among VMIs, and (2) each keV group versus the next incrementally to assess differences between consecutive VMIs. All multiple comparisons were done using pair t-tests and p values were corrected using the Bonferroni method. Relative differences between T3D and all VMI reconstructions were calculated using the formula: (VMImean - T3Dmean) / T3Dmean) * 100%.

4. Results

4.1 Results of plaque progression assessment

A total of 115 patients were enrolled (mean age 60.1 ± 9.6 years, 27% female). The average interval between the two CTA examinations was 2.6 ± 1.1 years. The mean effective radiation dose was 5.07 mSv at baseline and 5.09 mSv at follow-up (p=0.822). A total of 105 out of 115 patients (91.3%) exhibited CAD at baseline. The remaining 10 patients (8.7%) initially had no plaque, but developed minimal stenosis on follow-up (CAD-RADS 1). No progression of CAD was detected in 54 patients (46.7%).

Comparing the first and second coronary CTA images, significant increases were observed in SSS, SIS and CAD-RADS on the follow-up images: SSS: 4.63 ± 4.06 vs. 5.67 ± 5.10, p< 0.001; SIS: 3.43 ± 2.53 vs. 3.89 ± 2.65, p< 0.001; CAD-RADS 0: 8.7% vs. 0.0%, 1: 44.3% vs. 40.9%, 2: 34.8% vs. 40.9%, 3: 7.0% vs. 9.6%, 4: 3.5% vs. 6.1%, 5: 1.7% vs. 2.6%, p< 0.001 at baseline and follow-up, respectively.

The average annual progression rates were 0.41 ± 0.62 for SSS and 0.18 ± 0.34 for SIS. Progression in SSS, SIS, and CAD-RADS was observed in 53.0%, 29.6% and 28.7% of all cases, respectively. Notably, among patients without CAD-RADS progression during follow-up, 34.1% and 17.1% experienced progression in SSS and SIS, respectively (**Figure 1**). Among those who progressed based on SSS, only 54% showed changes

in CAD-RADS scores. This could potentially lead to a false impression that CAD had not progressed over time despite novel plaque development only reflected by SSS changes.

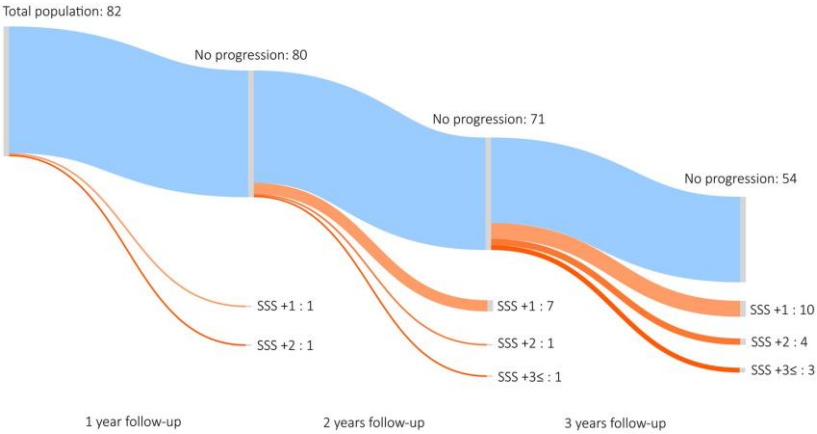

Figure 1. Sankey diagram depicting coronary plaque progression based on SSS among those with no progression in CAD-RADS classification for lesion severity. *(Source: Szilveszter B., Vattay B., et al. Eur Heart J Cardiovasc Imaging. 2022;23(11):1530-1539. CC BY 4.0)*

Multivariate analysis showed that smokers had a significantly increased annual progression rate of SSS by 0.37 per year [CI 0.07-0.67, p=0.017] and a higher total extent of CAD as described by SIS compared with non-smokers [β= 0.77, CI 0.06-1.50, p=0.034]. Diabetes mellitus increased the annual progression rate of SSS by 0.38 per year [CI: 0.07-0.69, p=0.016]. Age and gender affected the total amount of SSS and SIS ($p < 0.001$). Female gender was associated with an average of 2.86 lower SSS [CI -4.52-(-1.20), $p<0.001$] and 1.68 lower SIS [CI -2.65-(-0.71), p=0.001] compared to male gender.

Notably, CAD-RADS was not influenced by any cardiovascular risk factor (all p≥0.05).

4.2 Results of the association of quantitative plaque metrics and myocardial ischemia

A total of 30 patients were analyzed in the study (mean age 60.9 ± 8.3 years, 26.7% female). Common comorbidities included hypertension (76.7%) and dyslipidemia (76.7%). The average interval between the two examinations was 13.0 ± 8.6 days. The mean effective radiation dose was 4.4 ± 1.1 mSv for rest CTA and 8.9 ± 4.0 mSv for DPCT. Quantitative analysis was performed on 496 coronary artery segments and 480 myocardial segments. TPV, NCP volume, and CP volume differed significantly between ischemic and non-ischemic myocardial segments, measuring 120.5 ± 119.5 mm³ vs. 84.6 ± 82.2 mm³ (p=0.001), 62.3 ± 59.5 mm³ vs. 51.4 ± 54.9 mm³ (p=0.045), and 58.3 ± 91.8 mm³ vs. 33.3 ± 50.6 mm³ (p=0.001), respectively (**Figure 2**).

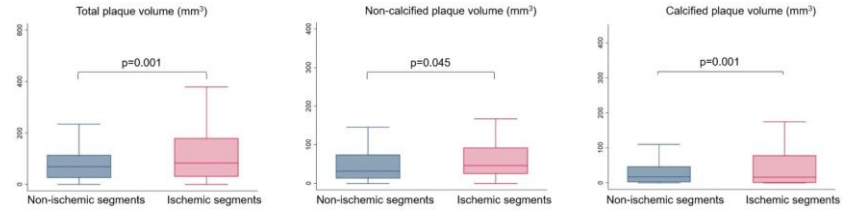

Figure 2. Box plots showing the distribution of total, NC and CP volumes related to ischemic and non-ischemic myocardial segments based on DPCT. *(Source: Vattay B., et al. Front Cardiovasc Med. 2022;9:974805. CC BY 4.0)*

On a segmental level, the average maximal lumen area stenosis was 37.2 ± 22.7% for ischemic segments and 33.5 ± 20.7% for non-ischemic segments (p=0.072). HRP was present in 21.3% of ischemic and 19.0% of non-ischemic territories (p=0.539).

The number of ischemic segments was 164 out of 480 (34.2%). The median MBF was 111 ml/100g/min, while the median relative MBF (MBFi) was 0.94. TPV strongly correlated with NCP volume ($r=0.73$, $p<0.001$) and CP volume ($r=0.83$, $p<0.001$); therefore, TPV was included in the multivariate prediction models to avoid multicollinearity.

Using linear mixed models, univariate analysis showed that total plaque volume predicted both absolute and relative MBF values. Clinical risk factors, HRP and stenosis severity were not associated with impaired MBF or MBFi. On multivariate analysis, an increase in TPV led to reduced MBF and MBFi values, even after adjusting for clinical risk factors, lumen area stenosis and HRP: per 10 mm^3 increase, $\beta= -0.035$, $p<0.01$ for MBF and $\beta= -0.0002$, $p<0.01$ for MBFi. Notably, lumen area stenosis and quantitative HRP features were not linked to absolute or relative MBF values (all $p>0.05$).

On multivariate logistic regression, after adjusting for clinical risk factors, stenosis severity and HRP, an increase in TPV was independently associated with myocardial ischemia: OR=1.01, $p=0.033$ (per 10 mm^3). However, HRP and lumen area stenosis were not linked to ischemia (both $p>0.05$).

4.3 Results of quantitative plaque characterization using photon-counting CT

A total of 51 plaques from 51 patients were included in the analyses. The average TPV was 270.2 ± 208.7 mm^3 on T3D images. The mean effective radiation dose was 5.2 ± 4.3 mSv. Using method 1 thresholds, the mean NCP volume was 161.0 ± 126.3 mm^3 on T3D images. The average NCP volume increased up to 70 keV and then decreased with each subsequent increment in VMI energy level. However, a significant difference in NCP volume between keV levels was not observed at every step. The lowest value was found using 40 keV, while

the highest was seen using 70 keV. Mean NCP volume measured on 100-180 keV reconstructions did not differ significantly from T3D images ($p>0.05$ for all) (**Figure 3A**). The average CP volume showed a significant graded decrease with increasing keV levels ($p<0.05$ for all) (**Figure 3B**). An increasing LAP volume was observed with each increment in keV level, showing a significant difference between each step ($p<0.0001$ for all). Mean LAP volumes differed significantly between T3D and VMI reconstructions, except for the 50 keV images ($p=0.63$) (**Figure 3C**). Method 2 yielded similar findings for plaque volume assessment. The mean NCP volume initially increased up to 100 keV and then decreased with higher keV levels, with no significant differences between each adjacent keV level. The average NCP volume on T3D was comparable to those at 70 and 140-180 keV energy levels ($p>0.05$ for all). Similarly, the mean CP volume showed a decreasing trend with significant differences between each adjacent keV level ($p<0.01$ for all). Mean CP volumes measured on each VMI reconstruction differed significantly from the reference T3D images ($p<0.001$ for all). Additionally, the LAP volume increased with higher keV levels, with significant difference between each adjacent VMI ($p<0.05$ for all). For LAP volume measurement, all VMIs showed significant differences compared to T3D, except for 40 keV images ($p=0.65$).

For plaque volumes using thresholds from method 1, the largest difference for CP and NCP volumes were observed on 40 keV images compared to T3D ($p<0.0001$). The smallest relative differences were found using 70 keV images ($p<0.0001$). The mean LAP volume showed the largest discrepancy on 180 keV reconstruction ($p<0.0001$), and the smallest on 50 keV images ($p=0.63$). Using method 2 for plaque quantification, the greatest difference in CP volume was between 180 keV and T3D ($p<0.0001$). The lowest relative difference of CP volume was on

70 keV images (p<0.001). For NCP volume compared to T3D, the greatest and smallest differences were found using 40 keV (p<0.0001) and 70 keV (p=0.54), respectively. The largest relative difference for LAP volume was seen on 180 keV images (p<0.0001), while the smallest on 40 keV images (p=0.65).

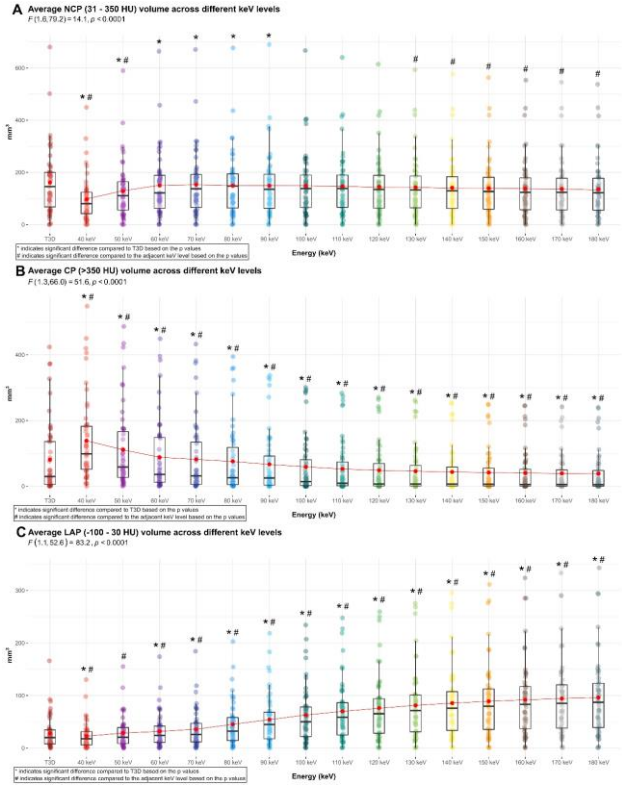

,

Figure 3. Box plots depicting the distribution of plaque volumes (method 1) in T3D images and different VMI energy levels. *(Source: Vattay B., et al. Eur Radiol. 2023;33(12):8528-8539. CC BY 4.0)*

5. Conclusions

In conclusion, this thesis addressed three critical aims to enhance CAD assessment using advanced coronary CTA and PCCT imaging. It showed that stenosis-based classifications like CAD-RADS may underestimate disease progression, that total plaque volume better predicts myocardial ischemia than stenosis severity, and that spectral imaging parameters significantly affect plaque quantification requiring new clinical standards. These insights pave the way for more accurate, reproducible and clinically meaningful evaluation of coronary atherosclerosis, potentially improving patient care through better risk stratification and targeted therapies.

6. Bibliography of the candidate's publications (Σ IF: 145.228)

6.1 Publications discussed in the present thesis (Σ IF: 14.6)

1. Szilveszter B*, **Vattay B***, Bossoussou M, Vecsey-Nagy M, Simon J, Merkely B, Maurovich-Horvat P, Kolossvary M. (2022) CAD-RADS may underestimate coronary plaque progression as detected by serial CT angiography. Eur Heart J Cardiovasc Imaging, 23: 1530-1539. **(SJR: D1; IF: 6.3)**
2. **Vattay B**, Borzsak S, Boussoussou M, Vecsey-Nagy M, Jermendy Á L, Suhai F I, Maurovich-Horvat P, Merkely B, Kolossvary M, Szilveszter B. (2022) Association between coronary plaque volume and myocardial ischemia detected by dynamic perfusion CT imaging. Front Cardiovasc Med, 9: 974805. **(SJR: Q1; IF: 3.6)**
3. **Vattay B**, Szilveszter B, Boussoussou M, Vecsey-Nagy M, Lin A, Konkoly G, Kubovje A, Schwarz F, Merkely B, Maurovich-Horvat P, Williams M C, Dey D, Kolossvary M. (2023) Impact of Virtual Monoenergetic Levels on Coronary Plaque Volume Components using Photon-Counting

Computed Tomography. Eur Radiol 33: 8528-8539 **(SJR: D1; IF: 4.7)**

4. **Vattay B**, Boussoussou M, Borzsák S, Vecsey-Nagy M, Simon J, Kolossváry M, Merkely B, Szilveszter B. (2021) Myocardial perfusion imaging using computed tomography: Current status, clinical value and prognostic implications. Imaging, 13: 49-60. **(SJR: Q4; IF: 0)**

6.2 Publications not related to the present thesis

1. Juhász D, Vecsey-Nagy M, Jermendy ÁL, Szilveszter B, Simon J, **Vattay B**, Boussoussou M, Dávid D, Maurovich-Horvát P, Merkely B, Apor A, Molnár L, Dósa E, Rakovics M, Johnson J, Manouras A, Nagy AI. (2025) Prognostic and therapeutic implications of a low aortic valve calcium score in patients with low-gradient aortic stenosis. Eur Heart J Cardiovasc Imaging. 26(2): 287-298.
2. Kravchenko D, Hagar MT, Vecsey-Nagy M, Tremamunno G, Szilveszter B, **Vattay B**, Zsarnóczay E, Beke S, Maurovich-Horvat P, Emrich T, Varga-Szemes A. (2025) Value of Ultrahigh-Resolution Photon-Counting Detector Computed Tomography in Cardiac Imaging. Echocardiography. 42(2): e70100.
3. Vecsey-Nagy M, Kolossváry M, Varga-Szemes A, Boussoussou M, **Vattay B**, Nagy M, Juhász D, Merkely B, Radovits T, Szilveszter B. (2024) Low-attenuation coronary plaque burden and troponin release in chronic coronary syndrome: A mediation analysis. J Cardiovasc Comput Tomogr. 18(1): 18-25.
4. Simon J, Hrenkó Á, Kerkovits NM, Nagy K, Vértes M, Balogh H, Nagy N, Munkácsi T, Emrich T, Varga-Szemes A, Boussoussou M, **Vattay B**, Vecsey-Nagy M, Kolossváry M, Szilveszter B, Merkely B, Maurovich-Horvat P. (2024) Photon-counting detector CT reduces the rate of referrals to

invasive coronary angiography as compared to CT with whole heart coverage energy-integrating detector. J Cardiovasc Comput Tomogr. 18(1): 69-74.
5. Weichsel L, Giesen A, André F, Renker M, Baumann S, Breitbart P, Beer M, Maurovitch-Horvat P, Szilveszter B, **Vattay B**, Buss SJ, Marwan M, Giannopoulos AA, Kelle S, Frey N, Korosoglou G. (2024) Comparison of Two Contemporary Quantitative Atherosclerotic Plaque Assessment Tools for Coronary Computed Tomography Angiography: Single-Center Analysis and Multi-Center Patient Cohort Validation. Diagnostics (Basel). 9;14(2):154.
6. **Vattay B**, Boussoussou M, Vecsey-Nagy M, Kolossváry M, Juhász D, Kerkovits N, Balogh H, Nagy N, Vértes M, Kiss M, Kubovje A, Merkely B, Maurovich Horvat P, Szilveszter B. (2024) Qualitative and quantitative image quality of coronary CT angiography using photon-counting computed tomography: Standard and Ultra-high resolution protocols. Eur J Radiol. 175: 111426.
7. Vecsey-Nagy M, Varga-Szemes A, Schoepf UJ, Tremamunno G, Fink N, Zsarnoczay E, Szilveszter B, Graafen D, Halfmann MC, **Vattay B**, Boussoussou M, O'Doherty J, Suranyi PS, Maurovich-Horvat P, Emrich T. (2024) Ultra-high resolution coronary CT angiography on photon-counting detector CT: bi-centre study on the impact of quantum iterative reconstruction on image quality and accuracy of stenosis measurements. Eur J Radiol. 176: 111517.
8. Sipos B, Vecsey-Nagy M, **Vattay B**, Boussoussou M, Jokkel Z, Borzsák S, Jermendy Á, Panajotu A, Gonda X, Rihmer Z, Merkely B, Szilveszter B, Nemcsik J. (2024) Association between affective temperaments and the severity and the extent of coronary artery disease as obtained by coronary CT angiography. J Affect Disord. 363: 47-54.

9. Weichsel L, André F, Renker M, Breitbart P, Overhoff D, Beer M, Giesen A, **Vattay B**, Buss S, Marwan M, Schlett CL, Giannopoulos AA, Kelle S, Frey N, Korosoglou G, Giusca S, Schütz M, Weberling LD, Schmitt R, Schoenberg SO, Kuru M, Klömpken S, Bálint Sz, Maurovich-Horvat P, Görich J, Emami M, Kaufmann PA, Doeblin P, Solowjawa N, Weiss KJ, Baumann S, Stach K, The LOCATE Investigators. (2024) Effects of high- versus low-intensity lipid-lowering treatment in patients undergoing serial coronary computed tomography angiography: results of the multi-center LOCATE study. Clin Res Cardiol.
10. Boussoussou M, **Vattay B**, Szilveszter B, Simon J, Lin A, Vecsey-Nagy M, Konkoly G, Merkely B, Maurovich-Horvat P, Dey D, Kolossváry M. (2023) The effect of patient and imaging characteristics on coronary CT angiography assessed pericoronary adipose tissue attenuation and gradient. J Cardiovasc Comput Tomogr. 17(1): 34-42.
11. Panajotu A, Vecsey-Nagy M, Jermendy ÁL, Boussoussou M, **Vattay B**, Kolossváry M, Dombrády ÖZs, Csobay-Novák Cs, Merkely B, Szilveszter B. (2023) Coronary CTA Amidst the COVID-19 Pandemic: A Quicker Examination Protocol with Preserved Image Quality Using a Dedicated Cardiac Scanner. Diagnostics (Basel) 13(3).
12. Vecsey-Nagy M, Jokkel Zs, Jermendy ÁL, Nagy M, Boussoussou M, **Vattay B**, Kolossváry M, Csobay-Novák Cs, Amin-Spector S, Merkely B, Szilveszter B. (2023) The Impact of Novel Reconstruction Algorithms on Calcium Scoring: Results on a Dedicated Cardiac CT Scanner. Diagnostics (Basel) 13(4).
13. Boussoussou M, Édes IF, Nowotta F, **Vattay B**, Vecsey-Nagy M, Drobni Z, Simon J, Kolossváry M, Németh B, Jermendy ÁL, Becker D, Leipsic J, Rogers C, Collinsworth A, Maurovich-Horvat P, Merkely B, Szilveszter B. (2023)

Coronary CT-based FFR in patients with acute myocardial infarction might predict follow-up invasive FFR: The XPECT-MI study. J Cardiovasc Comput Tomogr. 17(4): 269-276.
14. Vecsey-Nagy M, Varga-Szemes A, Emrich T, Zsarnóczai E, Nagy N, Fink N, Schmidt B, Nowak T, Kiss M, **Vattay B**, Boussouss M, Kolossváry M, Kubovje A, Merkely B, Maurovich-Horvat P, Szilveszter B. (2023) Calcium scoring on coronary computed angiography tomography with photon-counting detector technology: Predictors of performance. J Cardiovasc Comput Tomogr 17(5): 328-335.
15. Nagy FT, Olajos D, **Vattay B**, Borzsák S, Boussoussou M, Deák M, Vecsey-Nagy M, Sipos B, Jermendy ÁL, Tóth GG, Nemes B, Merkely B, Szili-Török T, Ruzsa Z, Szilveszter B. (2023) Dynamic Perfusion Computed Tomography for the Assessment of Concomitant Coronary Artery Disease in Patients with a History of Percutaneous Transluminal Angioplasty for Chronic Limb-Threatening Ischemia-A Pilot Study. J Cardiovasc Dev Dis. 10(11): 443.
16. Juhász D, **Vattay B**, Boussoussou M, Vecsey-Nagy M, Jokkel Zs, Jermendy ÁL, Merkely B, Édes IF, Szilveszter B. (2023) Korszerű koronáriaintervenció CT-vezérléssel: terápiás tervezés és előnyök. CARDIOLOGIA HUNGARICA 53: 571-576.
17. Simon J, Herczeg Sz, Borzsák S, Csőre J, Kardos AS, Mérges G, Zsarnóczay E, Szegedi N, Boussoussou M, **Vattay B**, Kolossváry M, Szilveszter B, Gellér L, Merkely B, Maurovich-Horvat P. (2022) Extracardiac findings on cardiac computed tomography in patients undergoing atrial fibrillation catheter ablation. Imaging 14: 52-59.
18. Boussoussou M, Szilveszter B, **Vattay B**, Kolossváry M, Vecsey-Nagy M, Salló Z, Orbán G, Perge P, Piros K, Nagy KV, Osztheimer I, Maurovich-Horvat P, Merkely B, Gellér

L, Szegedi N. (2022) The effect of left atrial wall thickness and pulmonary vein sizes on the acute procedural success of atrial fibrillation ablation. Int J Cardiovasc Imaging 38(7): 1601-1611.
19. Vecsey-Nagy M, Szilveszter B, Kolossváry M, Boussoussou M, **Vattay B**, Merkely B, Maurovich-Horvat P, Radovits T, Nemcsik J. (2022) Correlation between Coronary Artery Calcium- and Different Cardiovascular Risk Score-Based Methods for the Estimation of Vascular Age in Caucasian Patients. J Clin Med 11(4).
20. **Vattay B**, Nagy A I, Apor A, Kolossváry M, Manouras A, Vecsey-Nagy M, Molnár L, Boussoussou M, Bartykowszki A, Jermendy ÁL, Kováts T, Zsarnóczay E, Maurovich-Horvat P, Merkely B, Szilveszter B. (2022) The Predictive Value of Left Atrial Strain Following Transcatheter Aortic Valve Implantation on Anatomical and Functional Reverse Remodeling in a Multi-Modality Study. Front Cardiovasc Med 9: 841658.
21. Vecsey-Nagy M, Szilveszter B, Kolossváry M, Boussoussou M, **Vattay B**, Gonda X, Rihmer Z, Merkely B, Maurovich-Horvat P, Nemcsik J. (2022) Cyclothymic affective temperament is independently associated with left ventricular hypertrophy in chronic hypertensive patients. J Psychosom Res 160: 110988.
22. Vecsey-Nagy M, Jermendy ÁL, Kolossváry M, **Vattay B**, Boussoussou M, Suhai FI, Panajotu A, Csőre J, Borzsák S, Fontanini DM, Csobay-Novák Cs, Merkely B, Maurovich-Horvat P, Szilveszter B. (2022) Heart Rate-Dependent Degree of Motion Artifacts in Coronary CT Angiography Acquired by a Novel Purpose-Built Cardiac CT Scanner. J Clin Med 11(15).
23. Papp S, Bárczi Gy, Karády J, Kolossváry M, Drobni ZsD, Simon J, Boussoussou M, **Vattay B**, Szilveszter B,

Jermendy Gy, Merkely B, Maurovich-Horvat P. (2021) Coronary plaque burden of the left anterior descending artery in patients with or without myocardial bridge: A case-control study based on coronary CT-angiography. Int J Cardiol 327: 231-235.
24. Piros E A, Szilveszter B, **Vattay B**, Maurovich-Horvat P, Szalai K, Dósa E, Merkely B, Holló P. (2021) Novel anti-inflammatory therapies to reduce cardiovascular burden of psoriasis. Dermatol Ther 34(1): e14721.
25. Boussoussou M, **Vattay B**, Szilveszter B, Kolossváry M, Simon J, Vecsey-Nagy M, Merkely B, Maurovich-Horvat P. (2021) Functional assessment of coronary plaques using CT based hemodynamic simulations: current status, technical principles and clinical value. Imaging 13: 37-48.
26. Vecsey-Nagy M, Szilveszter B, Kolossváry M, Boussoussou M, **Vattay B**, Gonda X, Rihmer Zs, Merkely B, Maurovich-Horvat P, Nemcsik J. (2021) The association between accelerated vascular aging and cyclothymic affective temperament in women. J Psychosom Res 145: 110423.
27. Stengl R, Ágg B, Szilveszter B, Benke K, Daradics N, Ruskó B, **Vattay B**, Merkely B, Pólos M, Szabolcs Z. (2021) Case Report: Morphological Characterization and Long-Term Observation of Bilateral Sequential Internal Mammary Artery Aneurysms in a Patient With Confirmed FBN1 Mutation. Front Cardiovasc Med 8: 697591.
28. Vecsey-Nagy M, Szilveszter B, Kolossváry M, Boussoussou M, **Vattay B**, Gonda X, Rihmer Z, Merkely B, Maurovich-Horvat P, Nemcsik J. (2021) Association between affective temperaments and severe coronary artery disease. J Affect Disord 295: 914-919.
29. Vecsey-Nagy M, Jermendy ÁL, Suhai FI, Panajotu A, Csőre J, Borzsák S, Fontanini D M, Kolossváry M, **Vattay B**, Boussoussou M, Csobay-Novák Cs, Merkely B, Maurovich-

Horvat P, Szilveszter B. (2021) Model-based adaptive filter for a dedicated cardiovascular CT scanner: Assessment of image noise, sharpness and quality. Eur J Radiol 145: 110032.

30. Szilveszter B, Oren D, Molnár L, Apor A, Nagy A, Molnár A, **Vattay B**, Kolossváry M, Karády J, Bartykowszki A, Jermendy Á L, Suhai F I, Panajotu A, Maurovich-Horvat P, Merkely B. (2020) 1. Subclinical leaflet thrombosis is associated with impaired reverse remodelling after transcatheter aortic valve implantation. Eur Heart J Cardiovasc Imaging, 21(10): 1144-1151.
31. Szilveszter B, Nagy A I, **Vattay B**, Apor A, Kolossváry M, Bartykowszki A, Simon J, Drobni Z D, Tóth A, Suhai F I, Merkely B, Maurovich-Horvat P. (2020). Left ventricular and atrial strain imaging with cardiac computed tomography: Validation against echocardiography. J Cardiovasc Comput Tomogr 14(4): 363-369.
32. Simon J, Szaraz L, Szilveszter B, Panajotu A, Jermendy Á L, Bartykowszki A, Boussoussou M, **Vattay B**, Drobni ZD, Merkely B, Maurovich-Horvat P, Kolossvary M. (2020). Calcium scoring: a personalized probability assessment predicts the need for additional or alternative testing to coronary CT angiography. Eur Radiol 30(10): 5499-5506.